

Strong enhancement of third harmonic generation in a double layer graphene system caused by electron-hole pairing

K. V. GERMASH¹ and D. V. FIL^{1,2}

¹ *Institute for Single Crystals, National Academy of Sciences of Ukraine, Nauki ave. 60, Kharkov 61001, Ukraine*

² *V. N. Karazin Kharkov National University, Svobody Sq. 4, Kharkov 61022, Ukraine*

PACS 78.67.-n – Optical properties of low-dimensional, mesoscopic, and nanoscale materials and structures

PACS 42.65.Ky – Frequency conversion; harmonic generation, including higher-order harmonic generation

PACS 74.78.-w – Superconducting films and low-dimensional structures

Abstract – A manifestation of electron-hole pairing in nonlinear electromagnetic response of a double layer graphene system is studied. It is shown that the pairing causes the appearance of a number of peaks in the frequency dependence of the intensity of the third harmonic generation (THG). The highest peak corresponds to $\hbar\omega = (2/3)\Delta$, where ω is the incident wave frequency, and Δ is the order parameter of the electron-hole pairing. The absolute value of the THG intensity in the systems with electron-hole pairing is in several orders of magnitude greater than the THG intensity in the unpaired state. It is shown that huge enhancement of the THG intensity occurs both in the double monolayer and double bilayer graphene systems.

Introduction. – Nonlinear optical and microwave properties of graphene attract considerable attention. Strong nonlinear response of graphene can be seen from the classical equation of motion for a charged particle with the spectrum linear in the momentum [1,2]. This equation yields the electric current that contains all odd Fourier harmonics with the amplitudes falling down very slowly with the harmonic number. The quantum approach [3–7] predicts resonant behavior for the third harmonic generation in graphene. The frequency dependence of the THG intensity has the main peak at $\hbar\omega = (2/3)\varepsilon_F$ and two minor peaks at $\hbar\omega = \varepsilon_F$ and $\hbar\omega = 2\varepsilon_F$, where ε_F is the Fermi energy. Nonlinear optical effects in graphene systems were observed experimentally. In [8] the coherent nonlinear optical response of single- and few-layer graphene was measured using four-wave mixing. Sharp contrast images of graphene flakes on a dielectric substrate at combined frequencies were observed. Graphene with the effective thickness 3 \AA demonstrates the nonlinear emission intensity in 10 times larger than a 4 nm gold film. Nonlinear susceptibility at the wavelength $\lambda \approx 1 \text{ \mu m}$ is evaluated as large as 10^{-7} esu. In the THG experiment [9] the effective nonlinear susceptibility $\chi^{(3)} \sim 5 \cdot 10^{-9}$ esu at the incident wavelength $\lambda_i = 1.7 \text{ \mu m}$ was registered. Strong THG in a monolayer graphene on an amorphous silica substrate was

reported in [10]. It was shown that the effective nonlinear susceptibility of graphene is in 4.6 times larger than of a thick Au film (for $\lambda_i = 789 \text{ nm}$).

It is known that linear optical properties of graphene are also quite unusual. In a wide frequency range the absorption coefficient A of pristine graphene is determined by the fundamental constants: $A = \pi e^2 / \hbar c$ [11]. In a doped graphene the absorption is suppressed in the frequency range $\hbar\omega < 2\varepsilon_F$ due to the reduction of the interband transitions.

Graphene double layer systems are considered as perspective ones for achieving the electron-hole pairing. The electron-hole pairing is an analog of the Cooper pairing. It may reveal itself in a so-called counterflow superconductivity. The effect can also be understood as the superfluidity of a gas of electron-hole pairs. The possibility of electron-hole pairing in a double monolayer graphene (DMLG) system was considered in [12–15]. The pairing in DMLG in the quantum Hall regime was analyzed in [16–18]. In [19] we have considered electromagnetic properties of DMLG in the paired state and find resonant behavior of the absorption and reflection coefficients at the photon energy equal to the excitonic energy gap in the spectrum ($\hbar\omega = 2\Delta$).

The general idea of the electron-hole pairing in double

layer systems was put forward in [20, 21] well before the proposals [12–15]. The electron-hole pairing in quantum Hall systems was predicted in [22–24]. The pairing was registered in double quantum well AlGaAs heterostructures in the quantum Hall state under study of their transport properties [25–28]. The possibility of electron-hole pairing was also considered with reference to topological insulator heterostructures [29–32], double bilayer graphene [33], double few-layer graphene [34], transition metal dichalcogenide [35–37] and black phosphorene [38] double layers. Recently several experimental efforts to register electron-hole pairing in double layer graphene systems were done [39–42], but the results of these experiments are controversial.

The electron-hole pairing is caused by the Coulomb attraction. The bare Coulomb interaction is a strong one, but screening reduces this interaction that may result in a lowering of the critical (superfluid transition) temperature down to the μK range [43]. At the same time the pairing suppresses the screening [44]. Mutual influence of pairing and screening was analyzed in [45, 46]. It was found that the behavior of the system is very sensitive to the value of the dimensionless parameter r_s , the ratio of the average Coulomb interaction energy to the Fermi energy. For the monolayer graphene this parameter is a material constant independent of the density of carriers: $r_s = e^2/\hbar v_F \varepsilon_{eff}$, where v_F is the graphene Fermi velocity, and ε_{eff} is the effective dielectric constant (for a double-layer system on a dielectric substrate $\varepsilon_{eff} = (\varepsilon + 1)/2$, where ε is the substrate dielectric constant). According to [45], the screening is suppressed and the critical temperature reaches $T_c \sim 0.1\varepsilon_F$, if the parameter r_s exceeds the critical value $r_s^{(c)} \approx 1.5$. This condition is fulfilled at $\varepsilon_{eff} \lesssim 1.5$. It may correspond, for instance, a porous dielectric substrate with $\varepsilon \approx 2$ [47]. For the bilayer graphene the parameter r_s depends on the density of carriers: $r_s = (a_B^* k_F)^{-1}$, where k_F is the Fermi wave number, $a_B^* = \hbar^2 \varepsilon_{eff}/m_{eff} e^2$ is the effective Bohr radius and m_{eff} is the electron effective mass. In double bilayer graphene (DBLG) systems the screening is suppressed at $r_s > r_s^{(c)} \approx 5$, and since r_s increases under decrease in k_F , the latter condition can be achieved for crystalline dielectric substrates ($\varepsilon \approx 4$) as well.

Intensity of THG in a double layer system. –

The system under study consists of two monolayer or two bilayer graphene sheets (layers) separated by a thin dielectric layer. We imply that the concentration of conducting electrons in one layer is equal to the concentration of holes in the other layer. The incident wave with the frequency ω induces high frequency electric currents in the graphene layers. The component of the current that oscillates with the frequency 3ω is responsible for THG. Taking into account the electron-hole symmetry one can write nonlinear in the electric field current as

$$j_+^{(3)} = \sigma_{+++}^{(3)} E_+^3 + \sigma_{+--}^{(3)} E_+ E_-^2,$$

$$j_-^{(3)} = \sigma_{---}^{(3)} E_-^3 + \sigma_{-++}^{(3)} E_- E_+^2, \quad (1)$$

where $j_{\pm}^{(3)} = j_1^{(3)} \pm j_2^{(3)}$, $E_{\pm} = E_1 \pm E_2$, j_i is the electric current in the layer i and E_i is the electric field in this layer. Eqs. (1) are presented in the symbolic form. In the general case they are matrix integral equations that account tensor nature of the conductivity and nonlocality of the response in time and space. In the case of uncoupled layers (unpaired electrons and holes) the conductivities in (1) are expressed through $\sigma_1^{(3)}$, the 3rd order single-layer conductivity: $\sigma_{+++}^{(3)} = \sigma_{---}^{(3)} = \sigma_1^{(3)}/4$, $\sigma_{+--}^{(3)} = \sigma_{-++}^{(3)} = 3\sigma_1^{(3)}/4$.

In this study we put $E_- = 0$ due to the following reason. The ratio of amplitudes of the fields E_- and E_+ is evaluated as $|E_-|/|E_+| \approx q_z d/2$, where q_z is the normal component of the wave vector of the incident wave, and d is the interlayer distance. We consider the frequency range $\hbar\omega \lesssim \varepsilon_F$. In this range $|E_-|/|E_+| \lesssim k_F d v_F/c$, where c is the velocity of light. The electron-hole pairing occurs at rather small interlayer distance d . In particular, for the double monolayer graphene the condition $dk_F \lesssim 0.1$ should be fulfilled [45]. Therefore $|E_-|/|E_+| < 10^{-3}$ and nonlinear response to the small field E_- can be neglected.

Let the electric component of the incident wave is $E_x(z, t) = E_0 \cos(q_z z - \omega t)$. Then, the 3rd harmonic of the electric current is given by the expression

$$j_{x,+}^{(3\omega)}(t) = \sigma_{+++}^{(3)}(\omega, \omega, \omega) E_0^3 e^{-3i\omega t} + c.c., \quad (2)$$

where $\sigma_{+++}^{(3)}(\omega, \omega, \omega)$ is the $xxxx$ component of the high-frequency nonlinear conductivity tensor.

The boundary conditions determine the relation between the current (2) and the magnetic component of the generated wave. It yields

$$B_y^{(3)}(z, t) = \mp \frac{2\pi}{c} \sigma_{+++}^{(3)}(\omega, \omega, \omega) E_0^3 e^{\pm 3iq_z z - 3i\omega t} + c.c., \quad (3)$$

where sign \pm corresponds to different half-spaces. The boundary condition (3) assumes that the double layer system is considered as a zero-thickness conducting layer. It is equivalent to the limit $q_z d \rightarrow 0$.

The intensity of the third harmonic is given by the Poynting vector averaged over the period T :

$$I^{(3)} = \frac{c}{4\pi T} \int_0^T |\mathbf{E}^{(3)} \times \mathbf{B}^{(3)}| dt. \quad (4)$$

Assuming, for simplicity, that the dielectric constant of the environment is $\varepsilon = 1$, we obtain

$$I^{(3)} = 4 \left(\frac{2\pi}{c} \right)^4 |4\sigma_{+++}^{(3)}(\omega, \omega, \omega)|^2 I_{inc}^3, \quad (5)$$

where I_{inc} is the intensity of the incident wave. For two uncoupled layers ($\sigma_{+++}^{(3)} = \sigma_1^{(3)}/4$) Eq. (5) corresponds to the quadruplicate intensity of a single layer. The factor 4 is due to the constructive interference.

Electron-hole pairing in the double layer graphene. – In what follows we use the Dirac Hamiltonian that describes electromagnetic properties of graphene in the low-energy approximation. In this approximation two valleys near Dirac points K and K' are considered independently and each valley has two spin components. Each Dirac component yields the same contribution into the nonlinear conductivity. Below we consider only one component and take into account the other ones by the factor 4 in the final answer.

The Hamiltonian of the DMLG system has the form

$$H = \sum_{i,\mathbf{k},\lambda} \xi_{i\mathbf{k}\lambda} c_{i,\mathbf{k},\lambda}^+ c_{i,\mathbf{k},\lambda} + \frac{1}{2S} \sum_{i,j,\mathbf{q}} V_{ij}(q) : \hat{n}_{i,\mathbf{q}} \hat{n}_{j,-\mathbf{q}} : + \frac{1}{S} \sum_{i,\mathbf{q}} e\varphi_{i,\mathbf{q}}(t) \hat{n}_{i,-\mathbf{q}}, \quad (6)$$

where $c_{i,\mathbf{k},\lambda}^+(c_{i,\mathbf{k},\lambda})$ is the creation (annihilation) operator for the electron in the layer i in the state with the momentum \mathbf{k} and the subband index $\lambda = \pm 1$. This state corresponds to the energy $\xi_{i\mathbf{k}\lambda} = \varepsilon_{\mathbf{k}\lambda} - \mu_i$, where $\varepsilon_{\mathbf{k}\lambda} = \lambda \hbar v_F k$ is the electron spectrum of the monolayer graphene near K and K' point, and μ_i is the chemical potential in the layer i . In what follows we imply $\mu_1 = -\mu_2 = \mu$ and neglect the difference between μ and ε_F . In the Hamiltonian (6) $\hat{n}_{i,\mathbf{q}}$ is the electron density operator, $V_{ij}(q)$ is the Fourier component of the Coulomb interaction energy between electrons in the layers i and j , $\varphi_{i,\mathbf{q}}(t)$ is the Fourier component of the scalar potential of the external electromagnetic field, the notation $: \hat{O} :$ indicates the normal ordering of creation and annihilation operators, and S is the area of the system. The explicit expression for the electron density operator reads

$$\hat{n}_{i,\mathbf{q}} = \sum_{\mathbf{k},\lambda,\lambda'} g_{\mathbf{k}+\mathbf{q},\lambda',\mathbf{k},\lambda} c_{i,\mathbf{k}+\mathbf{q},\lambda'}^+ c_{i,\mathbf{k},\lambda}, \quad (7)$$

where

$$g_{\mathbf{k}_1,\lambda_1,\mathbf{k}_2,\lambda_2} = \frac{e^{\frac{i}{2}(\vartheta_{\mathbf{k}_1} - \vartheta_{\mathbf{k}_2})} + \lambda_1 \lambda_2 e^{-\frac{i}{2}(\vartheta_{\mathbf{k}_1} - \vartheta_{\mathbf{k}_2})}}{2} \quad (8)$$

and $\vartheta_{\mathbf{k}}$ is the angle between \mathbf{k} and the x -axis.

In (6) we use the gauge in which the vector potential is directed normally to the layers and the in-plane electric field is given by the scalar potential $E_x = -\partial\varphi/\partial x$. Such a gauge can be used if the x component (q_x) of the wave vector of the incident wave is nonzero. The response at normal incidence can be computed as the limit $q_x \rightarrow 0$.

The order parameter for the electron-hole pairing is given by the equation

$$\Delta_{\mathbf{k}\lambda} = \frac{1}{S} \sum_{\mathbf{q},\lambda'} V_{12}(q) \frac{1 + \lambda\lambda' \cos(\vartheta_{\mathbf{k}+\mathbf{q}} - \vartheta_{\mathbf{k}})}{2} \times \overline{\langle c_{1,\mathbf{k}+\mathbf{q},\lambda'}^+ c_{2,\mathbf{k}+\mathbf{q},-\lambda'} \rangle}. \quad (9)$$

The average in (9) is defined as $\overline{\langle \dots \rangle} = \text{Tr}(\hat{\rho} \dots)$, where $\hat{\rho}$ is the density matrix. This average is nonzero in the state in

which the number of electrons in one layer and the number of holes in the other layer are indefinite, and, in this sense, it can be considered as the anomalous average.

The mean-field Hamiltonian has the form

$$H_{MF}(t) = H_0 + H_{int}(t), \quad (10)$$

where

$$H_0 = \sum_{\mathbf{k},\lambda} \left[\xi_{\mathbf{k}\lambda} \left(c_{1,\mathbf{k},\lambda}^+ c_{1,\mathbf{k},\lambda} - c_{2,\mathbf{k},-\lambda}^+ c_{2,\mathbf{k},-\lambda} \right) - \left(\Delta_{\mathbf{k}\lambda} c_{2,\mathbf{k},-\lambda}^+ c_{1,\mathbf{k},\lambda} + H.c. \right) \right], \quad (11)$$

$$H_{int}(t) = \frac{1}{2S} \sum_{\mathbf{q}} e\varphi_{+,\mathbf{q}}(t) \hat{n}_{+,-\mathbf{q}}, \quad (12)$$

$\xi_{\mathbf{k}\lambda} = \varepsilon_{\mathbf{k}\lambda} - \mu$, $\varphi_+ = \varphi_1 + \varphi_2$, and $\hat{n}_+ = \hat{n}_1 + \hat{n}_2$. Due to the same reason as for E_- we put $\varphi_- = \varphi_1 - \varphi_2 = 0$ in Eq. (12).

It is known that in conventional superconductors the order parameter fluctuations influence the linear and nonlinear response to the external electromagnetic field [48, 49]. Nevertheless, in (12) we do not account such fluctuations. The reason is the following. In the case of the electron-hole pairing the order parameter fluctuations are coupled with the field φ_- . The field φ_- induces the fluctuations of the anomalous average in (9) that in its turn induces the variation of the difference of electron densities in the layers n_- . It results in a renormalization of the linear and nonlinear response to the field φ_- . On the contrary, the field φ_+ is decoupled from the amplitude and phase fluctuations of the order parameter, and the response to the field φ_+ is not modified under accounting the order parameter fluctuations.

To proceed further we apply the $u-v$ transformation that diagonalizes the Hamiltonian H_0 . The transformation reads

$$\begin{aligned} c_{1,\mathbf{k},\lambda} &= u_{\mathbf{k}\lambda} a_{\alpha,\mathbf{k},\lambda} + v_{\mathbf{k}\lambda} a_{\beta,\mathbf{k},\lambda}, \\ c_{2,\mathbf{k},-\lambda} &= u_{\mathbf{k}\lambda} a_{\beta,\mathbf{k},\lambda} - v_{\mathbf{k}\lambda} a_{\alpha,\mathbf{k},\lambda}, \end{aligned} \quad (13)$$

where $a_{\alpha(\beta),\mathbf{k},\lambda}$ are new second quantization operators that satisfy Fermi anticommutation relations. The coefficients in (13) are expressed as

$$u_{\mathbf{k}\lambda} = \sqrt{\frac{1}{2} \left(1 + \frac{\xi_{\mathbf{k}\lambda}}{E_{\mathbf{k}\lambda}} \right)}, \quad v_{\mathbf{k}\lambda} = \sqrt{\frac{1}{2} \left(1 - \frac{\xi_{\mathbf{k}\lambda}}{E_{\mathbf{k}\lambda}} \right)}, \quad (14)$$

where $E_{\mathbf{k}\lambda} = \sqrt{\xi_{\mathbf{k}\lambda}^2 + \Delta_{\mathbf{k}\lambda}^2}$ are the eigenenergies of the Hamiltonian H_0 .

The transformation (13) reduces (11) and (12) to the form

$$H_0 = \sum_{\nu} E_{\nu} a_{\nu}^+ a_{\nu}, \quad (15)$$

$$H_{int}(t) = \frac{1}{2S} \sum_{\mathbf{q}} \sum_{\nu_1, \nu_2} e\varphi_{+,-\mathbf{q}}(t) \delta_{\mathbf{k}_2, \mathbf{k}_1 - \mathbf{q}} R_{\nu_1, \nu_2} a_{\nu_1}^+ a_{\nu_2}. \quad (16)$$

Here for the one-particle states we introduce the notation $\nu \equiv (\eta, \mathbf{k}, \lambda)$, where $\eta = \alpha(\beta)$ corresponds to the positive (negative) energy $E_{\alpha, \mathbf{k}, \lambda} = E_{\mathbf{k}\lambda}$ ($E_{\beta, \mathbf{k}, \lambda} = -E_{\mathbf{k}\lambda}$). The components of the matrix \mathbf{R} in (16) read

$$\begin{aligned} R_{\alpha, \mathbf{k}_1, \lambda_1, \alpha, \mathbf{k}_2, \lambda_2} &= R_{\beta, \mathbf{k}_1, \lambda_1, \beta, \mathbf{k}_2, \lambda_2} = \\ g_{\mathbf{k}_1, \lambda_1, \mathbf{k}_2, \lambda_2} (u_{\mathbf{k}_1 \lambda_1} u_{\mathbf{k}_2 \lambda_2} + v_{\mathbf{k}_1 \lambda_1} v_{\mathbf{k}_2 \lambda_2}), \\ R_{\alpha, \mathbf{k}_1, \lambda_1, \beta, \mathbf{k}_2, \lambda_2} &= -R_{\beta, \mathbf{k}_1, \lambda_1, \alpha, \mathbf{k}_2, \lambda_2} = \\ g_{\mathbf{k}_1, \lambda_1, \mathbf{k}_2, \lambda_2} (u_{\mathbf{k}_1 \lambda_1} v_{\mathbf{k}_2 \lambda_2} - v_{\mathbf{k}_1 \lambda_1} u_{\mathbf{k}_2 \lambda_2}). \end{aligned} \quad (17)$$

The DBLG system is treated analogously. The monolayer graphene spectrum is replaced with the bilayer one: $\varepsilon_{\mathbf{k}\lambda}^{(b)} = \lambda \hbar^2 k^2 / 2m_{eff}$, and the factor g is modified as

$$g_{\mathbf{k}_1, \lambda_1, \mathbf{k}_2, \lambda_2}^{(b)} = \frac{e^{i(\vartheta_{\mathbf{k}_1} - \vartheta_{\mathbf{k}_2})} + \lambda_1 \lambda_2 e^{-i(\vartheta_{\mathbf{k}_1} - \vartheta_{\mathbf{k}_2})}}{2}. \quad (18)$$

Nonlinear conductivity. – To compute nonlinear conductivity we use the density matrix approach [50]. The density matrix satisfies the Liouville -von Neumann equation

$$\frac{\partial \hat{\rho}(t)}{\partial t} = \frac{1}{i\hbar} [\hat{H}_{MF}(t), \hat{\rho}(t)] - \gamma (\hat{\rho}(t) - \hat{\rho}^{(0)}), \quad (19)$$

where $\hat{\rho}^{(0)}$ is the equilibrium density matrix, and γ is the phenomenological relaxation rate. The equilibrium density matrix is diagonal in the basis of eigenfunctions of the Hamiltonian (15)

$$(\hat{\rho}^{(0)})_{\nu, \nu'} = \delta_{\nu, \nu'} f_{\nu}, \quad (20)$$

where $f_{\nu} = [\exp(E_{\nu}/T) + 1]^{-1}$ is the Fermi-Dirac distribution function. The interaction with the external field is considered as a small perturbation and the density matrix is sought as the series

$$\hat{\rho} = \hat{\rho}^{(0)} + \hat{\rho}^{(1)} + \hat{\rho}^{(2)} + \hat{\rho}^{(3)} + \dots \quad (21)$$

The terms in the series (21) satisfy the recurrent equation

$$\begin{aligned} (\hat{\rho}^{(i)}(t))_{\nu, \nu'} &= \frac{1}{i\hbar} \int_{-\infty}^t dt' ([\hat{H}_{int}(t'), \hat{\rho}^{(i-1)}(t')])_{\nu, \nu'} \\ &\quad \times e^{i(\omega_{\nu, \nu'} + \gamma)(t' - t)}, \end{aligned} \quad (22)$$

where $\omega_{\nu, \nu'} = (E_{\nu} - E_{\nu'})/\hbar$.

Let the scalar potential in the graphene layers is equal to $\varphi(\mathbf{r}, t) = \varphi_0 \sin(q_x x - \omega t)$. It corresponds to the electric field of the incident wave $\mathbf{E} = \mathbf{E}_0 \cos(\mathbf{q}\mathbf{r} - \omega t)$, where $\mathbf{E}_0 = (E_{0x}, 0, E_{0z})$, $\mathbf{q} = (q_x, 0, q_z)$, and $E_{0x} = -q_x \varphi_0$. Nonlinear in φ_0 part of electron density oscillations is given by the equation

$$n_+^{(3)}(\mathbf{r}, t) = \text{Tr}[\hat{\rho}^{(3)}(t) \hat{n}_+(\mathbf{r})]. \quad (23)$$

The 3rd harmonic term in the electron density oscillations reads

$$n_+^{(3\omega)}(\mathbf{r}, t) = n_0^{(3\omega)} e^{3i(q_x x - \omega t)} + c.c., \quad (24)$$

where the explicit expression for $n_0^{(3\omega)}$ can be obtained from Eq. (23). Using the continuity equation $e\partial n_+/\partial t + \nabla \mathbf{j}_+ = 0$ one finds

$$\mathbf{j}_{x,+}^{(3\omega)}(\mathbf{r}, t) = \frac{e\omega n_0^{(3\omega)}}{q_x} e^{3i(q_x x - \omega t)} + c.c. \quad (25)$$

Eqs. (23)-(25) yield the following expression for the current

$$\mathbf{j}_{x,+}^{(3\omega)}(\mathbf{r}, t) = e^{3i(q_x x - \omega t)} \sigma_{+++}^{(3)}(\mathbf{q}_x, \mathbf{q}_x, \mathbf{q}_x; \omega, \omega, \omega) E_{0x}^3 + c.c., \quad (26)$$

where

$$\begin{aligned} \sigma_{+++}^{(3)}(\mathbf{q}_x, \mathbf{q}_x, \mathbf{q}_x; \omega, \omega, \omega) &= -i \frac{e^4 \omega}{2S q_x^4} \\ &\times \sum_{\nu_1, \nu_2, \nu_3, \nu_4} \delta_{\mathbf{k}_2, \mathbf{k}_1 + \mathbf{q}_x} \delta_{\mathbf{k}_3, \mathbf{k}_2 + \mathbf{q}_x} \delta_{\mathbf{k}_4, \mathbf{k}_3 + \mathbf{q}_x} R_{12} R_{23} R_{34} R_{41} \\ &\quad \times \frac{1}{E_1 - E_4 - 3\hbar\omega - i\hbar\gamma} \left[\frac{1}{E_1 - E_3 - 2\hbar\omega - i\hbar\gamma} \right. \\ &\quad \times \left(\frac{f_1 - f_2}{E_1 - E_2 - \hbar\omega - i\hbar\gamma} - \frac{f_2 - f_3}{E_2 - E_3 - \hbar\omega - i\hbar\gamma} \right) \\ &\quad \left. - \frac{1}{E_2 - E_4 - 2\hbar\omega - i\hbar\gamma} \right] \\ &\quad \times \left(\frac{f_2 - f_3}{E_2 - E_3 - \hbar\omega - i\hbar\gamma} - \frac{f_3 - f_4}{E_3 - E_4 - \hbar\omega - i\hbar\gamma} \right) \end{aligned} \quad (27)$$

is the 3rd order nonlinear conductivity. In Eq. (27) the shorthand notations $E_i \equiv E_{\nu_i}$, $f_i \equiv f_{\nu_i}$, and $R_{ik} \equiv R_{\nu_i, \nu_k}$ are used. The factor 4 that accounts the sum over 4 Dirac components is included in (27). Taking the limit $q_x \rightarrow 0$ we arrive at the relations (2) and (5) with $\sigma_{+++}^{(3)}(\omega, \omega, \omega) = \lim_{q_x \rightarrow 0} \sigma_{+++}^{(3)}(\mathbf{q}_x, \mathbf{q}_x, \mathbf{q}_x; \omega, \omega, \omega)$.

Results and discussion. – It was shown in [13] that in a DMLG system the order parameter $\Delta_{\mathbf{k}, \lambda}$ is peaked at the Fermi surface and decreases far from this surface. In DBLG system a regime with almost constant $\Delta_{\mathbf{k}, \lambda}$ at $k < 4k_F$ was found in [33]. In our computations of THG intensity we neglect the wave vector dependence of the order parameter and replace $\Delta_{k_F, \lambda}$ with $\Delta = E_g/2$, where E_g is the energy gap. Such an approximation works well near the Fermi surface. The resonant features in the THG intensity described below are caused, in the main part, by the transitions between the electron states near the Fermi surface. It justifies the use of the approximation $\Delta_{k_F, \lambda} = \Delta$.

We fix the temperature and the relaxation rate as $T = 0.1\mu$ and $\hbar\gamma = 0.001\mu$. The ratio of the THG intensity to the incident wave intensity versus the incident wave frequency is shown in Figs. 1 and 2. Fig. 1 corresponds to the DMLG system and Fig. 2, to the DBLG system. The dependencies are presented for the paired state for two different values of the order parameter and for the unpaired state ($\Delta = 0$). The absolute value of the ratio $I^{(3)}/I_{inc}$ in Figs. 1 and 2 is computed for $\mu = 0.01$ eV and $I_{inc} = 5$ W/cm². The dependencies presented are scaled as

$$\frac{I^{(3)}}{I_{inc}} \propto \frac{I_{inc}^2}{\mu^8}$$

for the DMLG system, and

$$\frac{I^{(3)}}{I_{inc}} \propto \frac{I_{inc}^2}{\mu^6}$$

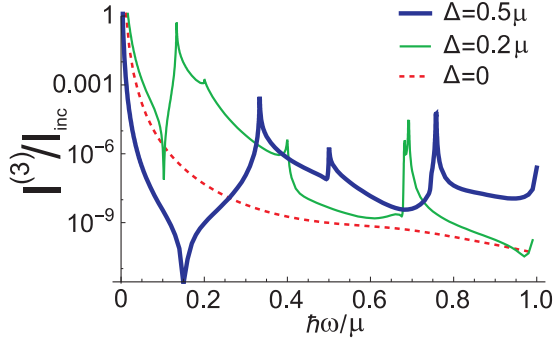


Fig. 1: THG intensity for the double monolayer graphene in the state with the electron-hole pairing ($\Delta = 0.5\mu, 0.2\mu$) and in the unpaired state ($\Delta = 0$)

for the DBLG system.

One can see that the dependencies obtained have a number of peaks. There are three peaks that correspond to the incident photon energies $\hbar\omega = (2/3)\Delta$, $\hbar\omega = \Delta$, and $\hbar\omega = 2\Delta$. Numerically the peaks appear because denominators in the expression for the nonlinear conductivity (27) become resonant when the incident photon energy $\hbar\omega$ exceeds $E_g/3$, $E_g/2$ and E_g . Physically, it means opening of new channels of nonlinear absorption. In addition a double peak emerges at $\hbar\omega \approx (2/3)\sqrt{\mu^2 + \Delta^2}$.

The peaks in THG intensity are rather sharp. We connect it with the divergence of the electron density of states in the paired state. Indeed, in the normal state the sum of the density of states in the electron and the hole layers is the constant $\nu_e + \nu_h = 2\nu_F$ in the interval $-\mu \leq \varepsilon \leq \mu$, where ν_F is the density of states at the Fermi level for a isolated monolayer (bilayer) graphene, and the energy ε is counted from the Fermi level. For the paired state simple calculations yield $\nu(\varepsilon) = 2\nu_F\varepsilon/\sqrt{\varepsilon^2 - \Delta^2}$ (in this case the density of states cannot be separated to the electron and the hole parts). This function diverges at $\varepsilon = \pm\Delta$. The influence of pairing on the spectrum and on the density of states in a DMLG system is illustrated in Fig. 3. Note that far from the Fermi level the energy spectra for the paired and the normal states approach each other. It means that the wave vector dependence of $\Delta_{\mathbf{k},\lambda}$ yields only an inessential correction of the spectrum that can be considered as another justification of the approximation $\Delta_{k_F,\lambda} = \Delta$.

The dependencies that correspond to $\Delta = 0$ do not demonstrate any peaks. The peaks predicted in [3, 4, 7] emerges at lower temperature ($T \lesssim 10^{-2}\mu$). Under transition to the normal state the double peak at $\hbar\omega \approx (2/3)\sqrt{\mu^2 + \Delta^2}$ is transformed to the peak at $\hbar\omega = (2/3)\mu$, and the peaks at $\hbar\omega = (2/3)\Delta$, $\hbar\omega = \Delta$, and $\hbar\omega = 2\Delta$ disappear.

One can see that the electron-hole pairing causes a huge increase of the intensity of THG in a certain frequency range. At the main peak $\hbar\omega = (2/3)\Delta$ the THG intensity is in 8 orders of magnitude greater than one for the

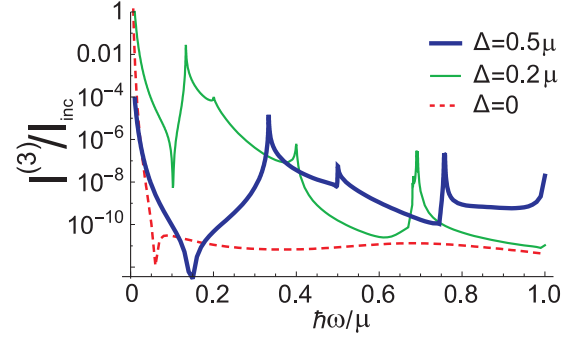


Fig. 2: The same as in Fig. 1 for the double bilayer graphene

unpaired state. For the out-of-resonance frequencies the factor of THG enhancement is also very large (about 10^3). We note that the enhancement of THG is not observed at large ($\hbar\omega \gg \Delta$) frequencies and at small ($\hbar\omega \ll \Delta$). In the latter case the pairing even suppresses the THG. It can be understood from the classical picture of a tightly bound electron-hole pair that does not respond to a static electric field if the same field is applied to the electron and the hole component of the pair.

Thus we consider that the enhancement of THG intensity is physically caused by the appearance of new resonant frequencies connected with the gap $E_g = 2\Delta$, and by the divergence of the density of states near the gap.

From the practical point of view the enhancement means that strong nonlinear response in the double layer graphene with electron-hole pairing can be observed at much smaller incident wave intensity than in the system where the pairing does not occur.

In conclusion, we have shown that the electron-hole pairing in the double layer graphene system results in the strong enhancement of the nonlinear response to the electromagnetic radiation. We predict the appearance of a number of peaks in the THG intensity. The main peak corresponds to the frequency equals to one third of the energy gap in the spectrum and the intensity of this peak exceeds in many orders the THG intensity at the same frequency in the unpaired state. The impact of the pairing is basically the same for the double monolayer and double bilayer graphene systems and we expect THG enhancement in other systems in which the electron-hole pairing may occur.

This work was supported by the State Fund for Fundamental Research of Ukraine, project No 33683.

REFERENCES

- [1] MIKHAILOV S. A., *Europhys. Lett.*, **79** (2007) 27002.
- [2] MIKHAILOV S. A. and ZIEGLER K., *J. Phys.: Condens. Matter*, **20** (2008) 384204.
- [3] MIKHAILOV S. A., *Phys. Rev. B*, **90** (2014) 241301(R).

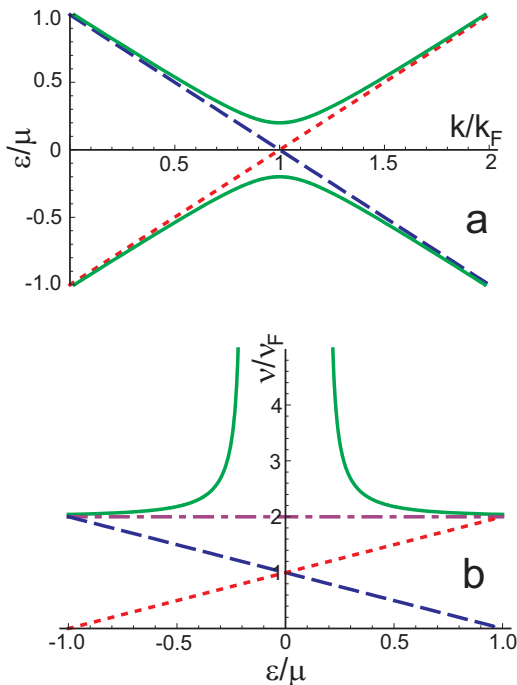


Fig. 3: Energy spectrum (a) and density of states (b) near the Fermi level in a double monolayer graphene for the paired state with $\Delta = 0.2\mu$ (solid lines) and for the normal state (dotted lines, dashed and dash-dotted lines). Dotted lines correspond to the electron-doped graphene layer, and dashed lines, to the hole-doped one. The total (electron plus hole) density of states is shown by the dash-dotted line. The energy difference between the Dirac points in the electron and hole layers is equal 2μ . The energy ε is counted from the Fermi level, and the wave vector k is counted from the Dirac point.

- [4] MIKHAILOV S. A., *Phys. Rev. B*, **93** (2016) 085403.
 [5] CHENG J. L., VERMEULEN N. and SIPE J. E., *New J. Phys.*, **16** (2014) 053014.
 [6] CHENG J. L., VERMEULEN N. and SIPE J. E., *Phys. Rev. B*, **91** (2015) 235320.
 [7] ROSTAMI H. and POLINI M., *Phys. Rev. B*, **93** (2016) 161411(R).
 [8] HENDRY E., HALE P. J., MOGER J., SAVCHENKO A. K. and MIKHAILOV S. A., *Phys. Rev. Lett.*, **105** (2010) 097401.
 [9] KUMAR N., KUMAR J., GERSTENKORN C., WANG R., CHIU H.-Y., SMIRL A. L. and ZHAO H., *Phys. Rev. B*, **87** (2013) 121406(R).
 [10] HONG S.-Y., DADAP J. I., PETRONE N., YEH P.-C., HONE J. and OSGOOD JR R. M., *Phys. Rev. X*, **3** (2013) 021014.
 [11] NAIR R. R., BLAKE P., GRIGORENKO A. N., NOVOSELOV K. S., BOOTH T. J., STAUBER T., PERES N. M. R. and GEIM A. K., *Science*, **320** (2008) 1308.
 [12] LOZOVIK YU. E. and SOKOLIK A. A., *Pisma Zh. Eksp. Teor. Fiz.*, **87** (2008) 61; *JETP Lett.*, **87** (2008) 55.
 [13] ZHANG C.-H. and JOGLEKAR Y. N., *Phys. Rev. B*, **77** (2008) 233405.
 [14] MIN H., BISTRITZER R., SU J.-J. and MACDONALD A. H., *Phys. Rev. B*, **78** (2008) 121401(R).
 [15] SERADJEH B., WEBER H. and FRANZ M., *Phys. Rev. Lett.*, **101** (2008) 246404.
 [16] BERMAN O. L., LOZOVIK Y. E. and GUMBS G., *Phys. Rev. B*, **77** (2008) 155433.
 [17] FIL D. V. and KRAVCHENKO L. YU., *Fiz. Nizk. Temp.*, **35** (2009) 904; *Low Temp. Phys.*, **35** (2009) 712.
 [18] PIKALOV A. A. and FIL D. V., *Nanoscale Res. Lett.*, **7** (2012) 145.
 [19] GERMASH K. V. and FIL D. V., *Phys. Rev. B*, **93** (2016) 205436.
 [20] SHEVCHENKO S. I., *Fiz. Nizk. Temp.*, **2** (1976) 505; *Sov. J. Low Temp. Phys.*, **2** (1976) 251.
 [21] LOZOVIK YU. E. and YUDSON V. I., *Zh. Eksp. Teor. Fiz.*, **71** (1976) 738; *Sov. Phys. JETP*, **44** (1976) 389.
 [22] FERTIG H. A., *Phys. Rev. B*, **40** (1989) 1087.
 [23] YOSHIOKA D. and MACDONALD A. H., *J. Phys. Soc. Jpn.*, **59** (1990) 4211.
 [24] MOON K., MORI H., YANG K., GIRVIN S. M., MACDONALD A. H., ZHENG L., YOSHIOKA D. and ZHANG S. C., *Phys. Rev. B*, **51** (1995) 5138.
 [25] KELLOGG M., EISENSTEIN J. P., PFEIFFER L. N. and WEST K. W., *Phys. Rev. Lett.*, **93** (2004) 036801.
 [26] WIERSMA R. D., LOK J. G. S., KRAUS S., DIETSCH W., VON KLITZING K., SCHUH D., BICHLER M., TRANITZ H.-P. and WEGSCHEIDER W., *Phys. Rev. Lett.*, **93** (2004) 266805.
 [27] TUTUC E., SHAYEGAN M. and HUSE D. A., *Phys. Rev. Lett.*, **93** (2004) 036802.
 [28] NANDI D., FINCK A. D. K., EISENSTEIN J. P., PFEIFFER L. N. and WEST K. W., *Nature*, **488** (2012) 481.
 [29] SERADJEH B., MOORE J. E. and FRANZ M., *Phys. Rev. Lett.*, **103** (2009) 066402.
 [30] CHO G. Y. and MOORE J. E., *Phys. Rev. B*, **84** (2011) 165101.
 [31] EFIMKIN D. K., LOZOVIK YU. E. and SOKOLIK A. A., *Phys. Rev. B*, **86** (2012) 115436.
 [32] GERMASH K. V. and FIL D. V., *Phys. Rev. B*, **87** (2013) 115313.
 [33] PERALI A., NEILSON D. and HAMILTON A. R., *Phys. Rev. Lett.*, **110** (2013) 146803.
 [34] ZARENIA M., PERALI A., NEILSON D. and PEETERS F. M., *Sci. Rep.*, **4** (2014) 7319.
 [35] FOGLER M. M., BUTOV L. V. and NOVOSELOV K. S., *Nature Commun.*, **5** (2014) 4555.
 [36] WU F.-C., XUE F. and MACDONALD A. H., *Phys. Rev. B*, **92** (2015) 165121.
 [37] BERMAN O. L. and KEZERASHVILI R. YA., *Phys. Rev. B*, **93** (2016) 245410.
 [38] BERMAN O. L., GUMBS G. and KEZERASHVILI R. YA., *Phys. Rev. B*, **96** (2017) 014505.
 [39] GORBACHEV R. V., GEIM A. K., KATSNELSON M. I., NOVOSELOV K. S., TUDOROVSKIY T., GRIGORIEVA I. V., MACDONALD A. H., MOROZOV S. V., WATANABE K., TANIGUCHI T. and PONOMARENKO L. A., *Nat. Phys.*, **8** (2012) 896.
 [40] GAMUCCI A., SPIRITO D., CARREGA M., KARMAKAR B., LOMBARDO A., BRUNA M., PFEIFFER L. N., WEST K. W., FERRARI A. C., POLINI M. and PELLEGRINI V., *Nat. Commun.*, **5** (2014) 5824.
 [41] LI J. I. A., TANIGUCHI T., WATANABE K., HONE J., LEVCHENKO A. and DEAN C. R., *Phys. Rev. Lett.*, **117**

- (2016) 046802.
- [42] LEE K., XUE J., DILLEN D. C., WATANABE K., TANIGUCHI T. and TUTUC E., *Phys. Rev. Lett.*, **117** (2016) 046803.
- [43] KHARITONOV M. Y. and EFETOV K. B., *Phys. Rev. B*, **78** (2008) 241401(R).
- [44] GERMASH K. V. and FIL D. V., *Phys. Rev. B*, **91** (2015) 115442.
- [45] SODEMANN I., PESIN D. A. and MACDONALD A. H., *Phys. Rev. B*, **85** (2012) 195136.
- [46] LOZOVIK YU. E., OGARKOV S. L. and SOKOLIK A. A., *Phys. Rev. B*, **86** (2012) 045429.
- [47] VOLKSEN W., MILLER R. D. and DUBOIS G., *Chem. Rev.*, **110** (2010) 56.
- [48] KULIK I. O., ENTIN-WOHLMAN O. and ORBACH R., *J. Low Temp. Phys.*, **43** (1981) 591.
- [49] CEA T., CASTELLANI C. and BENFATTO L., *Phys. Rev. B*, **93** (2016) 180507(R).
- [50] BOYD R. W., *Nonlinear Optics. Third Edition* (Academic Press) 2008.